HHS Public Access

Author manuscript

J Occup Environ Hyg. Author manuscript; available in PMC 2020 September 04.

Published in final edited form as:

J Occup Environ Hyg. 2020 June ; 17(6): 301–311. doi:10.1080/15459624.2020.1742915.

Aerodynamic size separation of glass fiber aerosols

Taekhee Lee[a], **Bon Ki Ku**[b], **Rachel Walker**[a], **Pramod Kulkarni**[b], **Teresa Barone**[a], **Steven Mischler**[a]

[a]Dust, Ventilation, and Toxic Substances Branch, Pittsburgh Mining Research Division, National Institute for Occupational Safety and Health, Centers for Disease Control and Prevention, Pittsburgh, Pennsylvania;

[b]Chemical and Biological Monitoring Branch, Health Effects Laboratory Division, National Institute for Occupational Safety and Health, Centers for Disease Control and Prevention, Cincinnati, Ohio

Abstract

The objective of this study was to investigate the efficacy of an aerodynamic separation scheme for obtaining aerosols with nearly monodisperse fiber lengths as test samples for mechanistic toxicological evaluations. The approach involved the separation of aerosolized glass fibers using an Aerodynamic Aerosol Classifier (AAC) or a multi-cyclone sampling array, followed by the collection of separated samples on filter substrates, and the measurement of each sample fiber length distribution. A glass fiber aerosol with a narrow range of aerodynamic sizes was selected and sampled with the AAC or multi-cyclone sampling array in two separate setups. The fiber length and diameter were measured using a field emission scanning electron microscope. The glass fiber aerosol was separated in distinct groups of eight with the AAC and of four with the multi-cyclone sampling array. The geometric standard deviations of the fiber length distributions of the separated aerosols ranged from 1.49 to 1.69 for the AAC and from 1.6 to 1.8 for multi-cyclone sampling array. While the separation of glass fiber aerosols with an AAC is likely to produce two different length fiber groups and the length resolution may be acceptable, the overall mass throughput of these separation schemes is limited.

Keywords

Aerodynamic Aerosol Classifier; airborne fibers; asbestos; elongate mineral particles

CONTACT Taekhee Lee fwc8@cdc.gov Dust, Ventilation, and Toxic Substances Branch, Pittsburgh Mining Research Division, National Institute for Occupational Safety and Health, 626 Cochrans Mill Road, Pittsburgh, PA 15236.

Introduction

Health effects related to the exposure of elongate mineral particles (EMPs), which include the six types of regulated asbestos, have been well established in the literature (Wylie 2016; Cook et al. 2016; NIOSH 2011). During the mining and processing of mineral commodities and other rock types, EMPs can become airborne and be inhaled by mine workers. There is little information available on the extent to which mine workers may be exposed to EMPs based on the geologies of the materials being mined; however, the National Institute for Occupational Safety and Health (NIOSH) estimates that mining mineral commodities possibly containing EMPs may result in the exposure of 44,000 mine workers to some form of EMP, including asbestos fiber and amphibole cleavage fragments (NIOSH 2011). Both the Mine Safety and Health Administration (MSHA) and the Occupational Safety and Health Administration (OSHA) regulate six different types of airborne asbestos fibers in occupational environments, which are defined based on mineral type (one serpentine and five amphiboles) and crystallization in asbestiform habit. NIOSH (1994), OSHA (1997), and MSHA (2008) agree on exposure limits of less than 0.1 fiber/cc. NIOSH recommends that cleavage fragments from asbestos minerals, which are crystallized in massive form, be regulated as asbestos fibers, as long as they meet dimensional criteria (NIOSH 2011). However, these EMPs are not currently included as asbestos under MSHA and OSHA regulations. Fibers of winchite and richterite, which contaminate vermiculite (from Libby, MT), have health effects identical to asbestos. These fibers were formerly included within the definition of tremolite (one of the six types of regulated asbestos) but are no longer specifically named in OSHA and MSHA regulations. In addition, fibers of erionite, which cause asbestos-related diseases such as mesothelioma, are unregulated. A cytotoxic effect comparison between an asbestiform mineral (crocidolite) and a non-asbestiform analog (riebeckite) was made and both materials showed cytotoxicity (Castranova et al. 1994). It has been known that EMPs with high aspect ratio can be cleared by phagocytosis or persist and induce frustrated phagocytic interactions leading to diseases (Zeidler-Erdely et al. 2006; Padmore et al. 2017). Fiber diameters and lengths affecting disease pathogenesis and the asbestos exposure-related diseases were dependent on fiber dimension and dose (Lippmann 2014). The role of fiber length in determining the toxicity of EMPs is not yet fully understood. Toxicological evaluation with different length of EMPs is important, because retained EMPs in lungs can vary considerably between different fiber length intervals.

Baron and colleagues (Baron et al. 1994, 1998; Deye et al. 1999) developed Fiber Length Classifier (FLC) to classify aerosolized fibers and collect samples for toxicology studies. This FLC separates particles using dielectrophoretic force induced by a nonuniform electric field in an annular laminar flow field. Classification using the FLC showed good fiber length resolution. The glass fibers collected with the FLC have been studied to determine the role of fiber length in cytotoxicity (Zeidler-Erdely et al. 2006; Blake et al. 1998). However, the mass throughput of the FLC was too low to be practically useful; up to 1 mg/day could be collected, making it difficult to collect large mass to enable large-scale toxicological studies. Therefore, there is a continuing need for methods to classify or separate aerosolized fibers with high length resolution and high mass throughput.

The NIOSH Pittsburgh Mining Research Division is establishing a research effort to understand elongate mineral particle (EMP) exposures in the mining industry. One major task in this research effort is to find an optimal respirable size fraction of EMP (asbestos and non-asbestiform analogs) separation method with uniform (or similar) length parameters in terms of physical, chemical and surface reactivity properties. The present study was a preliminary trial to separate glass fiber aerosols aerodynamically with commercially available instruments to develop the method to collect EMPs in reasonably monodisperse distributions with a reasonable amount in number and weight of the separated EMPs. The objective of this study was to evaluate efficacy of aerodynamic separation scheme to obtain separated fiber samples with distinct fiber length distributions.

Materials and methods

Glass fiber powder (GW1), supplied by the Japan Fibrous Material Research Association (JFMRA) (Kohyama et al. 1997), was used as a surrogate for asbestos in this study. Two different methods were utilized for the aerodynamic classification of glass fiber aerosols: (1) the Aerodynamic Aerosol Classifier (AAC, Cambustion Ltd., Cambridge, UK) and (2) multi-cyclone sampling array with Higgins-Dewell type and sharp-cut cyclones.

Separation of glass fiber aerosols with the aerodynamic aerosol classifier

The AAC classifies airborne particles by relaxation time (s) and selects particles with a narrow range of aerodynamic diameters (Tavakoli and Olfert 2013; Tavakoli et al. 2014). The experimental setup for fiber separation using the AAC is shown in Figure 1. The glass fiber aerosol was generated using a vortex mixer shaking method that was described in detail previously (Ku et al. 2013, 2017). Briefly, the glass fiber powder was placed in a Pyrex tube that was fixed to a pop-off cup on a vortex mixer (Vortex-Genie 2, Scientific Industries Inc.). During vortex mixing, high-efficiency particulate air (HEPA) filtered air (1.0 L/min) was input through a port at the top of the tube for fiber suspension. The generated glass fiber aerosols were passed through a second port and conductive tubing that led to the inlet of the AAC. The operating conditions of the AAC are listed in Table 1, which includes selected size, cylinder rotation speed, sheath flow rate, and sample flow rate. The aerodynamic size distribution of separated glass fibers from the AAC was measured using an Aerodynamic Particle Sizer (APS, Model 3321, TSI Inc., Shoreview, MN). Three measurements were made for each selected size at the AAC outlet. The separated glass fiber aerosols were collected for further analysis using mixed cellulose ester filter (MCE; SKC Inc., Eighty Four, PA) and polycarbonate membrane (PC; 0.4-μm pore size, 25 mm, Sterlitech, Kent, WA, USA) filters mounted in a cowl sampler (225–321 A, SKC Inc.). The length of glass fiber aerosols separated by the AAC and collected on the MCE filter were inspected with a phase contrast microscope (PCM) for a rough estimate of fiber length. First, the MCE filter was cleared with an acetone vaporizing unit (QuickFix, RJ Lee Instrument Inc., Trafford, PA), and subsequently the length of the fibers was measured using a PCM with 400x magnification and Motic software (Motic Incorporation Ltd., Hong Kong). In addition, the classified glass fibers collected on PC filters were analyzed by field emission scanning electron microscopy (FESEM, model S-4800–2, Hitachi High Technologies America Inc.). Samples were prepared for FESEM analysis by placing PC filters in centrifugal tubes with 5

mL of isopropyl alcohol and extracting fibers from the PC filters using a combination of sonication and vortex mixing. Extracted glass fibers were deposited on another PC filter (0.4-μm pore size) using a borosilicate filtration apparatus (MilliporeSigma, Burlington, MA) and a vacuum pump. The PC filter was placed on a SEM specimen aluminum mount with a conductive carbon double-sided adhesive tape (SPI Supplies, West Chester, PA). The length and width of the classified glass fiber aerosols were examined by the FESEM.

Classification of glass fiber aerosols with the multi-cyclone sampling array

The multi-cyclone sampling array was previously employed for the size-segregation of crystalline silica for toxicological evaluations (Mischler et al. 2013, 2016). In this study, the same sampling array was utilized for the separation of glass fibers using the experimental setup shown in Figure 2. The system included two different cyclones and cowl sampler loaded with a PC filter in a series. The cyclones were a Higgins-Dewell (HD) type (BGI4L, Mesa Labs, Butler, NJ; cut off diameter (d_{50}): 4 μm at 2.2 L/min), and sharp-cut type (SCC) with a 0.74-mm cut size (SCC 0.695, Mesa Labs, Butler, NJ; d_{50}: 0.74 μm at 2.2 L/min) and a 0.38-μm cut size (SCC 0.695, Mesa Labs, d_{50}: 0.38 μm at 4.4 L/min). To match the final flow rate (4.4 L/min), two HD and SCC cyclones with 2.2 L/min were used in parallel. The glass fiber aerosol generation method was the same as that described in the section above. After sampling with the multi-cyclone array, the separated glass fiber aerosols were collected from: (a) two grit pots of HD cyclones (Stage 1); (b) two grit pots of SCC cyclones with 2.2 l/min (Stage 2); and (c) the grit pot of the SCC cyclone with 4.4 L/min (Stage 3). Material from each grit pot was collected separately by washing them with isopropyl alcohol and collecting the sample in conical centrifuge tubes (Fisher Scientific, Pittsburgh, PA). The PC filter from the cowl sampler (Stage 4) was directly placed on a SEM specimen aluminum mount with conductive carbon tape.

Fiber diameter and length measurements

Each sample was coated with a thin layer of gold/palladium utilizing a sputter coater (SPI Supplies, West Chester, PA). A sequence of fields was selected at random locations and an image of each field acquired. The length and width of approximately 300 fibers for each sample were manually measured with ImageJ software (Schneider et al. 2012).

Aerodynamic diameter calculation

Aerodynamic diameter was calculated to compare particle size distributions between separated glass fiber aerosols and APS measurement. The aerodynamic diameter may be a good criterion to determine respirable fraction of the fibers. Fiber aerodynamic diameter depends on the fiber physical dimensions [diameter (d_f) and length (L)] and on the orientation of the fiber in the measuring flow field (Cox 1970, Kulkarni et al. 2011). The aerodynamic diameter of the glass fiber aerosol was calculated with the fiber diameter and length measured by the FESEM using the following equations:

$$d_{ae,\parallel} = d_f \left\{ \frac{9\rho_f}{4\rho_0} [\ln(2\beta) - 0.807] \right\}^{1/2} \quad (1)$$

$$d_{ae,\perp} = d_f \left\{ \frac{9\rho_f}{8\rho_0} [\ln(2\beta) + 0.193] \right\}^{1/2}, \quad (2)$$

where $d_{ae,\parallel}$ is aerodynamic diameter when the fiber is parallel to relative gas motion, $d_{ae,\perp}$ is aerodynamic diameter when the fiber is aligned perpendicular to relative gas motion, $\beta = \frac{L}{d_f}$ is the aspect ratio, and ρ_f and ρ_0 are the fiber (2250 Kg/m^3) and unit densities, respectively. For random orientation, the aerodynamic diameter was calculated by:

$$d_{ae} = \frac{\left(d_{ae,\parallel} + 2d_{ae,\perp}\right)}{3}. \quad (3)$$

Results and discussion

Separation with the aerodynamic aerosol classifier

Phase contrast microscope images (400x magnification) of separated (selected AAC aerodynamic diameters of 1, 2, and 3 mm) and not separated glass fiber aerosols are shown in Figure 3. Most of the thick and long glass fibers in the nonseparated sample (Figure 3(d) were removed by the AAC as shown in Figure 3(a–c). Figure 4 shows (a) the normalized number-weighted distribution of glass fiber aerosols classified with the AAC in different selected particle sizes as a function of calculated aerodynamic diameter and (b) the cumulative number fraction of glass fibers. A significant difference between distributions was not found by the Mann-Whitney U test. Figure 5 shows (a) the normalized length-weighted distribution of glass fiber aerosols separated with the AAC as a function of fiber length and (b) the cumulative length fraction of glass fibers. The shortest group (AAC size selection 0.5 μm) showed significantly differences with longer groups (AAC size selection >1.25 μm) by the Mann-Whitney U test. Table 2 shows the aerodynamic diameter selected with the AAC, the number of the glass fibers analyzed with the FESEM, the geometric mean (GM) of the calculated aerodynamic diameters of the glass fibers using Equations (1)–(3), the geometric standard deviation (GSD, $\sigma = \frac{d_{84\%}}{d_{50\%}}$) of the aerodynamic diameter, the GM of glass fiber length, the σ of glass fiber length, the GM of glass fiber width, and the σ of glass fiber width. Table 3 shows average count median aerodynamic diameter (CMAD, average of three particle distributions), average σ, average number concentration, and average mass concentration measured with the APS for each selected size with the AAC. The average mass concentration was calculated using particle number concentration and density of the glass fiber aerosols. Selected aerodynamic diameter with AAC, the geometric mean diameter from FESEM analysis, and the CMAD from the APS are not significantly different each other by paired t-test ($p > 0.05$). The GM aerodynamic diameter of the separated glass fiber aerosols increased with an increased aerodynamic diameter selected with AAC. A positive and weak correlation was found between length and width of the glass fibers separated with AAC (Pearson correlation coefficient, $r = .285$, $p > 0.05$) indicating that longer fibers are thicker fibers.

Separation with multi-cyclone sampling array

Figure 6 shows (a) the normalized number-weighted distribution of glass fiber aerosols classified with the multi-cyclone sampling array as a function of calculated aerodynamic diameter and (b) the cumulative number fraction of glass fibers. Stages 1 and 4 showed significantly difference in their number-weighted distributions as a function of calculated aerodynamic diameter. Figure 7 shows (a) the normalized length-weighted distribution of glass fiber aerosols classified with the multi-cyclone sampling array as a function of fiber length and (b) the cumulative length fraction of glass fibers. Stages 1 and 4 showed significant difference in their number-weighted distributions as a function of fiber length. Table 4 shows the number of glass fibers analyzed with the FESEM, GM of the calculated aerodynamic diameters of the glass fibers, σ of the aerodynamic diameter, GM of glass fiber length, σ of glass fiber length, GM of glass fiber width, and σ of glass fiber width. A positive and moderate correlation was found between length and width of the glass fibers separated with multi-cyclone sampling array ($r = 0.583$, $p > 0.05$).

There have been several methods developed to separate EMPs by length or other characteristic of concern. The classification of the glass fiber aerosols using dielectrophoretic mobility (FLC) showed reasonably monodisperse distributions (Baron et al. 1994; Deye et al. 1999; Ku et al. 2013). The GSD of the classified glass fiber aerosols with FLC ranged from 1.19 to 1.35 in four different classifications of glass fibers by length (different applied voltages, 1–4 kV). Ku et al. (2014) investigated the use of various nylon net filters (10, 20, and 60-μm mesh sizes) to efficiently separate fibers based on their length and found that single screens were not particularly effective in separating long fibers; however, an alternative configuration, especially a centrally blocked screen configuration, yielded samples substantially free of the fibers. The GSDs ranged from 1.89 to 2.99 in different fiber length distributions obtained with nylon net screens. Padmore et al. (2017) developed a glass fiber separation method using a combination of crushing (high and low pressure for short and long fibers, respectively), sonication, and sedimentation. The study showed that the fiber length distributions were confirmed to be log-normal, where the mean physical length was 7.0 μm and 39.3 mm for short and long fibers, respectively. The GSDs of fiber length distributions from the present study are slightly larger than the Ku et al. (2017) study; GSDs from classification with the AAC ranged from 1.49 to 1.69 (Table 2), GSDs from the multi-cyclone sampling array ranged from 1.60–1.82 (Table 4), and GSDs from the Ku et al. study ranged from 1.19 to 1.35 when the glass fibers were separated using the FLC. The shortest length groups separated with the AAC (aerodynamic size 0.5 μm) and multi-cyclone sampling array (Stage 4) showed significant difference ($p > 0.05$).

An additional experiment was conducted to remove short fibers (<10 μm) from a separated fiber group (AAC selection 3.0 mm) using an electrostatic precipitator (ESP, custom made), DC power supply (model 3015B and EMCO high voltage converter (model 4100 N)). An aerosol neutralizer (Model 3087, TSI Inc.) and the ESP were connected to the inlet and outlet of the AAC, respectively. APS was connected to the outlet of the ESP to monitor the particle size distribution. The applied voltage ranged from 200 to 1,000 volts to allow removal of short fibers from the AAC aerosols. However, it was observed that the ESP removed both small and long fibers at the same time.

The number and mass concentration estimation of glass fibers classified with the AAC is based on the APS measurement (Table 3). The collection time can be estimated with those mass concentrations. For example, the mass concentration of the separated glass fibers with the AAC 3.0-μm size selection was 702 $\mu g/m^3$ and it would take approximately 17 hr to collect 702 μg. However, the inlet air of the APS was diluted in half with a HEPA filter (Figure 1). Thus, the mass concentration would be two times larger, which reduces the sampling time by half (8.5 hr) to collect 702 μg. The sampling flow and sheath flow rates of the AAC were 0.3 and 11.36 L/min (Table 1), respectively, and the mass concentration was diluted at the ratio of sampling flow to sheath flow rate. The sampling flow rate can be increased up to 1.5 L/min and sheath flow can be reduced, which might lower the resolution on the distribution.

The fiber dimensions (length and diameter) of interest for toxicological evaluation has been summarized. Early biological evidence showed that fiber length between 10 and 50 μm were related with the major asbestosis hazard and short fibers (shorter than 5 μm) were more effectively cleared from the lungs (Walton 1982). The NIOSH fiber counting “A” rule, which apples to fibers longer than 5 μm and aspect ratio greater than 3 originated from these findings. A report from the expert panel on health effects of asbestos and synthetic vitreous fibers: the influence of fiber length separated health effects on the short fibers (<5 μm) by types of health effects, i.e., cancer and noncancer effects (Eastern Research Group 2003). The report concluded that short fibers are not related to cancer in humans but may be pathogenic for pulmonary fibrosis. Later, Lippmann (2014) determined that the critical fiber diameters and lengths affecting disease pathogenesis and the critical fiber dimension were dependent on diseases: asbestosis (surface area if fibers with length > 2 μm, diameter > 0.15 μm), mesothelioma (number of fibers with length > 5 μm, diameter <0.1 μm), and lung cancer (number of fibers with length > 10 μm, diameter > 0.15 μm). Two different groups in different lengths for toxicological evaluations, longer than 5 mm and shorter than 5 μm, may be necessary but counting longer than 5 μm fiber was selected as the lower size limit for counting (a margin of safety) (Walton 1982; Langer et al. 1978). The respirable size fraction of fiber glass that was collected with the respirable size-selective sampler (Casella, Buffalo, NY) and horizontal elutriator (MRE type 113 A) was previously investigated using an APS without information of fiber diameter and length (Iles 1990). The present study showed that collection of EMPs in two different length groups might be achievable with the AAC for shorter than 10 μm and longer than 10 μm or shorter than 5 μm and longer than 5 μm. For example, more than 90% of separated glass fiber aerosols with AAC 0.5-μm size selection were shorter than 10 μm and about 20% of glass fiber aerosol with AAC 3.0-μm size selection were shorter than 10 μm within the limited fiber length measurements in the samples (approximately 300 fibers for each group). The smallest selected aerodynamic diameter with the AAC was 0.5 μm in the present study, but smaller aerodynamic diameter can be selected with the AAC to make a group of shorter fibers less than 10 μm (or 5 μm). Particle selection of the AAC ranges from 0.025 to 5 um. If median fiber length is shorter than glass fiber aerosols generated in the present study (about 18 μm), it is likely to collect a greater number of samples in a shorter period of time. Generally, size distribution of EMPs are log-normal indicating that shorter fibers are dominant (Chatfield 2018). Shorter fibers can be produced by more grinding of reference materials. However, it should be noted that

material preparation and manipulation of the reference materials, including ball milling, might change crystallinity, and reduced crystallinity might reduce biological activity (Langer et al. 1978; Spurny et al. 1979). A combination method for classification of the EMPs is also achievable using multi-cyclone sampling array followed by the AAC; EMPs might be separated using the multi-cyclone (operating in high flow rates) sampling array to eliminate long EMPs, and separated EMPs may be separated again with the AAC to reduce a burden in the separation process. The present study utilized glass fiber aerosols as a surrogate of asbestos, but the classification of the regulated asbestos and its non-asbestiform analogs may be necessary. Prior to the toxicology studies, the classified EMPs materials should be fully characterized.

Conclusions

Airborne glass fibers were separated aerodynamically with an AAC and multi-cyclone sampling array prior to the classification of elongate mineral particles including regulated asbestos. The glass fiber aerosol separated using the AAC showed a slightly narrower fiber length distribution compared to that separated with the multi-cyclone sampling array, although throughput from the multi-cyclone sampling array can be higher than that of AAC. Based on the findings from the present experimental study, the separation of glass fiber aerosols with an AAC is likely to produce two different length fiber groups with different aerodynamic size selection of the AAC and the production rate was similar to a previously published technique involving separation by dielectrophoretic mobility. The production rate or mass throughput may be further improved by increasing the sampling flow rate.

References

Baron PA, Deye GJ, Fernback J. 1994 Length separation of fibers. Aerosol Sci Technol. 21(2):179–192. doi:10.1080/02786829408959707

Baron PA, Gao P, Deye GJ, Maynard AC. 1998 Performance of a fiber length classifier. J Aerosol Sci. 29(Suppl.1):S11–S12. doi:10.1016/S0021-8502(98)00082-2

Blake T, Castranova V, Schwegler-Berry D, Baron P, Deye GJ, Li C, Jones W. 1998 Effect of fiber length on glass microfiber cytotoxicity. J Toxicol Environ Health Part A. 54(4):243–259. doi:10.1080/009841098158836 [PubMed: 9638898]

Castranova V, Pailes WH, Judy D, Schwegler BD, Jones W. 1994 Comparative cytotoxic effects of crocidolite and its non-asbestiform polymorph on rat alveolar marcrophages. Annals of Occupational Hygiene. 38(Supplement 1):665–673. doi:10.1093/annhyg/38.inhaled_particles_VII.665

Chatfield EJ. 2018 Measurement of elongate mineral particles: what we should measure and how do we do it. Toxicol Appl Pharmacol. 361:36–46. doi:10.1016/j.taap.2018.08.010 [PubMed: 30134140]

Cook PC, Swintek J, Dawson TD, Chapman D, Etterson MA, Hoff D. 2016 Quantitative structure – mesothelioma potency model optimization for complex mixtures of elongated particles in rat pleura: a retrospective study. J Toxicol Environ Health. Part B2016 19 (5–6):266–288. doi:10.1080/10937404.2016.1195326

Cox RG. 1970 The motion of long slender bodies in a viscous fluid I: general theory. J Fluid Mech. 44(04): 791–810. doi:10.1017/S002211207000215X

Deye GJ, Gao P, Baron PA, Fernback J. 1999 Performance evaluation of a fiber length classifier. Aerosol Sci Technol. 30(5):420–437. doi:10.1080/027868299304471

Eastern Research Group. 2003 Report on the expert panel on health effects of asbestos and synthetic vitreous fibers: the influence of fiber length.

Iles PJ. 1990 Size selection of fibres by cyclone and horizontal elutriator. J Aerosol Sci. 21(6):745–760. doi:10.1016/0021-8502(90)90040-5

Kohyama N, Tanaka I, Tomita M, Kudo M, Shinohara Y. 1997 Preparation and characteristics of standard reference samples of fibrous minerals for biological experiments. Ind Health. 35(3):415–432. doi:10.2486/indhealth.35.415 [PubMed: 9248227]

Ku BK, Deye G, Turkevich LA. 2013 Characterization of a vortex shaking method for aerosolizing fibers. Aerosol Sci Technol. 47(12):1293–1301. doi:10.1080/02786826.2013.836588 [PubMed: 26635428]

Ku BK, Deye G, Turkevich LA. 2017 Screen collection efficiency of airborne fibers with monodisperse length. J Aerosol Sci. 115:250–262. doi:10.1016/j.jaerosci.2017.09.006

Ku BK, Deye GJ, Turkevich LA. 2014 Efficacy of screens in removing long fibers from an aerosol stream-sample preparation technique for toxicology studies. Inhal Toxicol. 26(2):70–83. doi:10.3109/08958378.2013.854851 [PubMed: 24417374]

Kulkarni P, Baron PA, Willeke K. 2011 Aerosol measurement, principles, techniques, and applications. 3rd ed New York: John Wiley & Sons, Inc.

Langer AM, Wolff MS, Rohl AN, Selikoff IJ. 1978 Variation of properties of chrysotile asbestos subjected to milling. J Toxicol Environ Health. 4(1):173–188. doi:10.1080/15287397809529654 [PubMed: 204800]

Lippmann M 2014 Toxicological and epidemiological studies on effects of airborne fibers: coherence and public [corrected] health implications. Crit Rev Toxicol. 44(8): 643–695. doi:10.3109/10408444.2014.928266 [PubMed: 25168068]

[MSHA] Mine Safety and Health Administration. 2008 30 CFR Parts 56, 57, and 71 Asbestos exposure limit; final rule.

Mischler SE, Cauda EG, Di Giuseppe M, McWilliams LJ, St. Croix C, Sun M, Franks J, Ortiz LA. 2016 Differential activation of RAW 264.7 macrophages by size-segregated crystalline silica. J Occup Med Toxicol. 11:57doi:10.1186/s12995-016-0145-2 [PubMed: 28018477]

Mischler SE, Cauda EG, Giuseppe MD, Ortiz LA. 2013 A multi-cyclone sampling array for the collection of size-segregated occupational aerosols. J Occup Environ Hyg. 10(12):685–693. doi:10.1080/15459624.2013.818244 [PubMed: 24195535]

[NIOSH] National Institute for Occupational Safety and Health. 1994 Method 7400. In NIOSH Manual of analytical methods, 4th edition, Asbestos and other fibers by PCM. Cincinnati, OH: U.S. Department of Health and Human Services, Centers for Disease Control and Prevention, National Institute for Occupational Safety and Health.

[NIOSH] National Institute for Occupational Safety and Health. 2011 Asbestos fibers and other elongate mineral particles: state of the science and roadmap for research. Cincinnati, OH: U.S. Department of Health and Human Services, Centers for Disease Control and Prevention, National Institute for Occupational Safety and Health, Current Intelligence Bulletin 62. DHHS publication No. 2011–159.

[OSHA] Occupational Safety and Health Administration. 1997 Method ID-160, Asbestos in air, OSHA Salt Lake Technical Center, Sandy, UT.

Padmore T, Stark C, Turkevich LA, Champion JA. 2017 Quantitative analysis of the role of fiber length on phagocytosis and inflammatory response by alveolar macrophages. Biochim Biophys Acta Gen Subj. 1861(2):58–67. doi:10.1016/j.bbagen.2016.09.031 [PubMed: 27784615]

Schneider CA, Rasband WS, Eliceiri KW. 2012 NIH image to ImageJ: 25 years of image analysis. Nat Methods. 9(7): 671–675. doi:10.1038/nmeth.2089 [PubMed: 22930834]

Spurny KR, Stöber W, Opiela H, Weiss G. 1979 Size-selective preparation of inorganic fibers for biological experiments. Am Ind Hyg Assoc J. 40(1):20–38. doi:10.1080/15298667991429291 [PubMed: 484448]

Tavakoli F, Olfert JS. 2013 An instrument for the classification of aerosols by particle relaxation time: theoretical models of the aerodynamic aerosol classifier. Aerosol Sci Technol. 47(8):916–926. doi:10.1080/02786826.2013.802761

Tavakoli F, Symonds JPR, Olfert JS. 2014 Generation of a monodisperse size-classified aerosol independent of particle charge. Aerosol Sci Technol. 48(3):i–iv. doi:10.1080/02786826.2013.877121

Walton WH. 1982 The nature, hazards and assessment of occupational exposure to airborne asbestos dust: a review. Ann Occup Hyg. 25(2):117–247. doi:10.1093/annhyg/25.2.117 [PubMed: 6753691]

Wylie AG. 2016 Amphibole dusts: fibers, fragments, and mesothelioma. Can Mineral. 54(6):1403–1435. doi:10.3749/canmin.1500109

Zeidler-Erdely PC, Calhoun WJ, Ameredes BT, Clark MP, Deye GJ, Baron P, Jones W, Blake T, Castranova V. 2006 In vitro cytotoxicity of Manville Code 100 glass fibers: effect of fiber length on human alveolar macrophages. Part Fibre Toxicol. 3:5 doi:10.1186/1743-8977-3-5 [PubMed: 16569233]

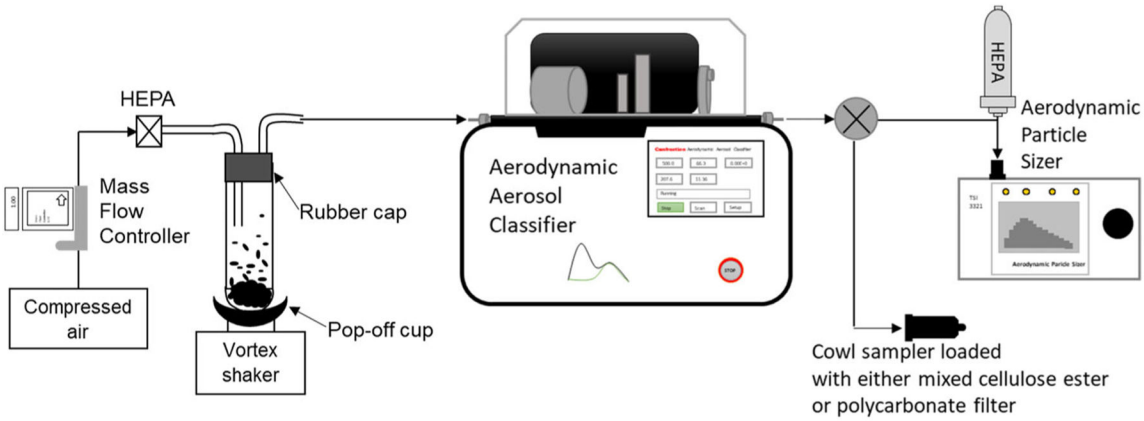

Figure 1.
Experimental setup for glass fiber aerosol separation with Aerodynamic Aerosol Classifier.

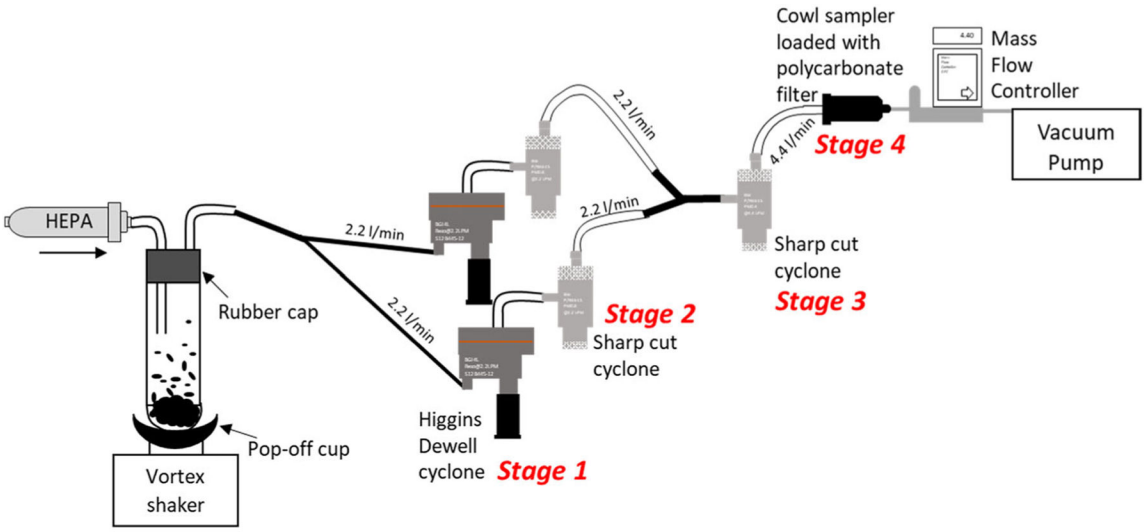

Figure 2.
Experimental setup for glass fiber aerosol separation with multi-cyclone sampling array.

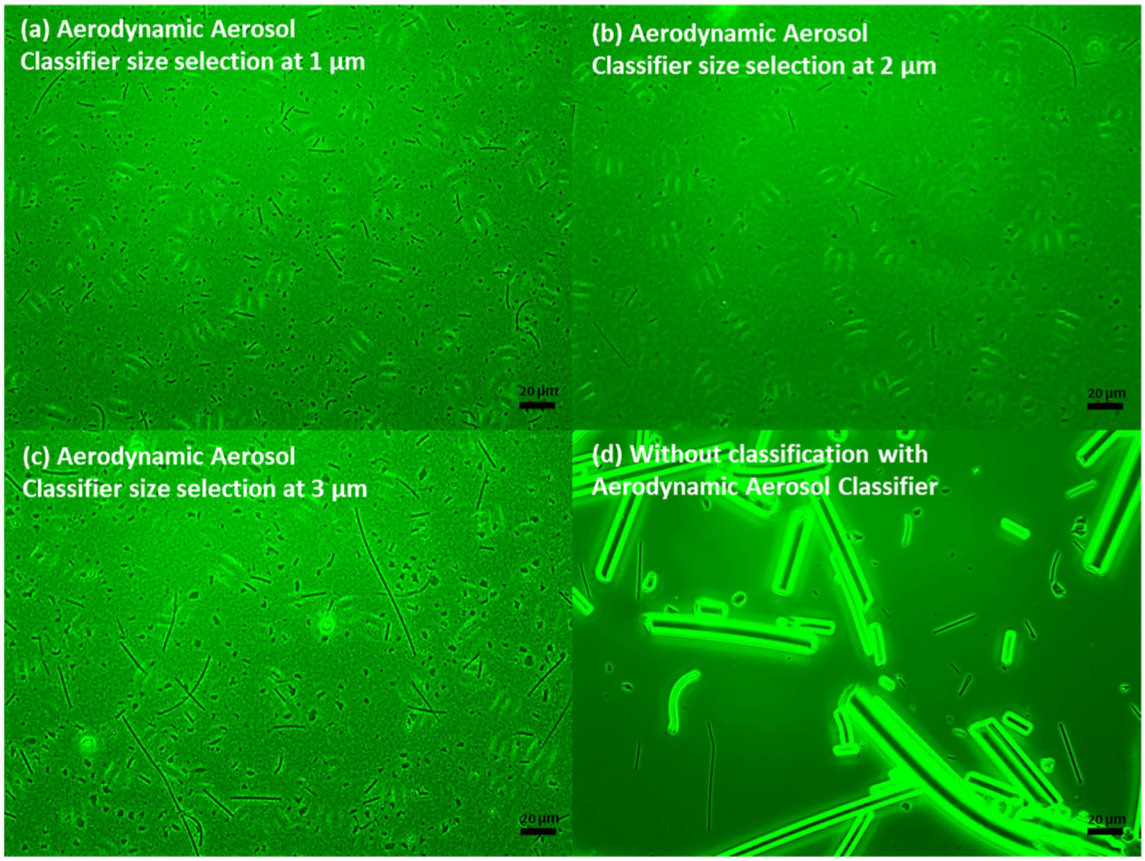

Figure 3.

Phase contrast microscope images (400x magnification) of glass fiber aerosols with the Aerodynamic Aerosol Classifier selected aerodynamic diameters of (a) 1 µm, (b) 2 µm, (c) 3 µm, and (d) without separation.

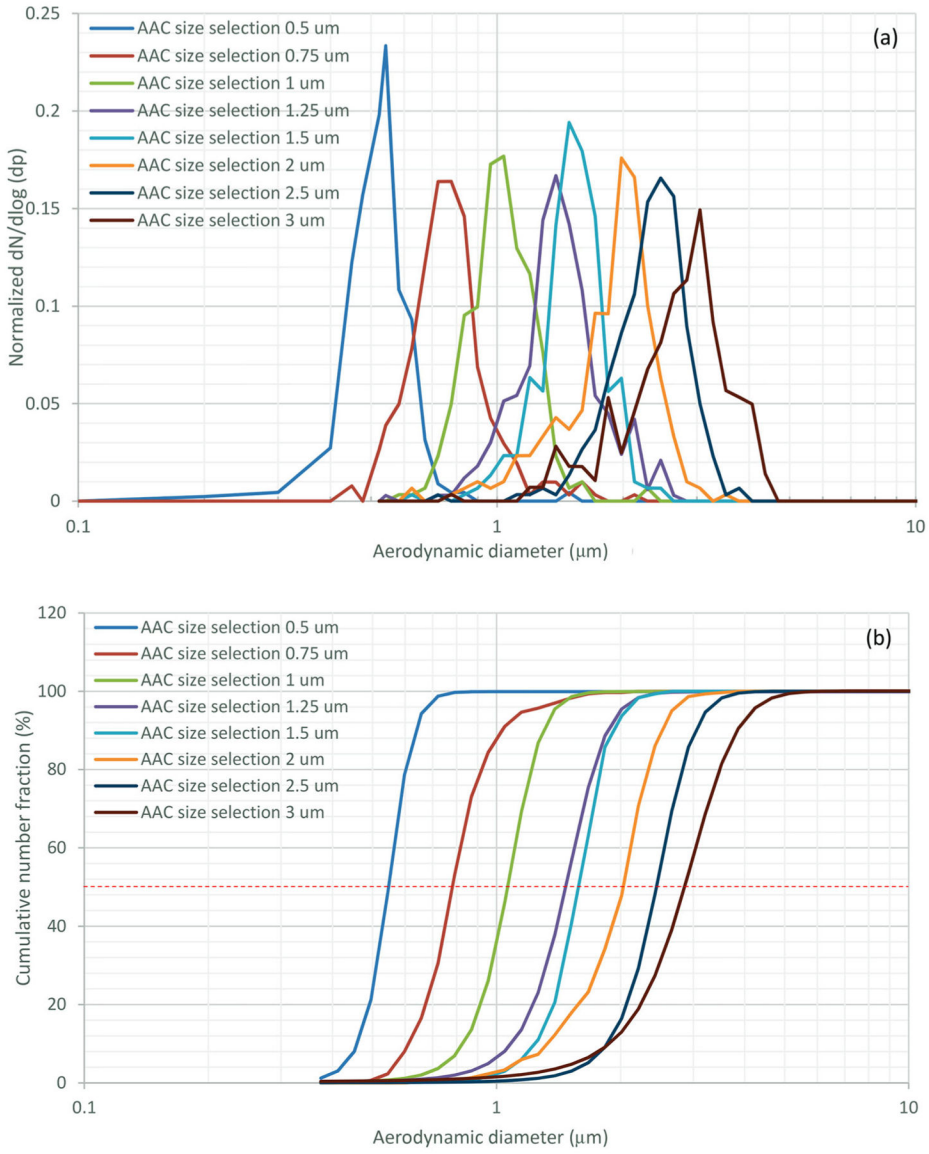

Figure 4.

Normalized particle number-weighted distribution of glass fiber aerosols between Aerodynamic Aerosol Classifier size selection (a) and cumulative number distribution for aerodynamic diameter of glass fiber aerosols (b).

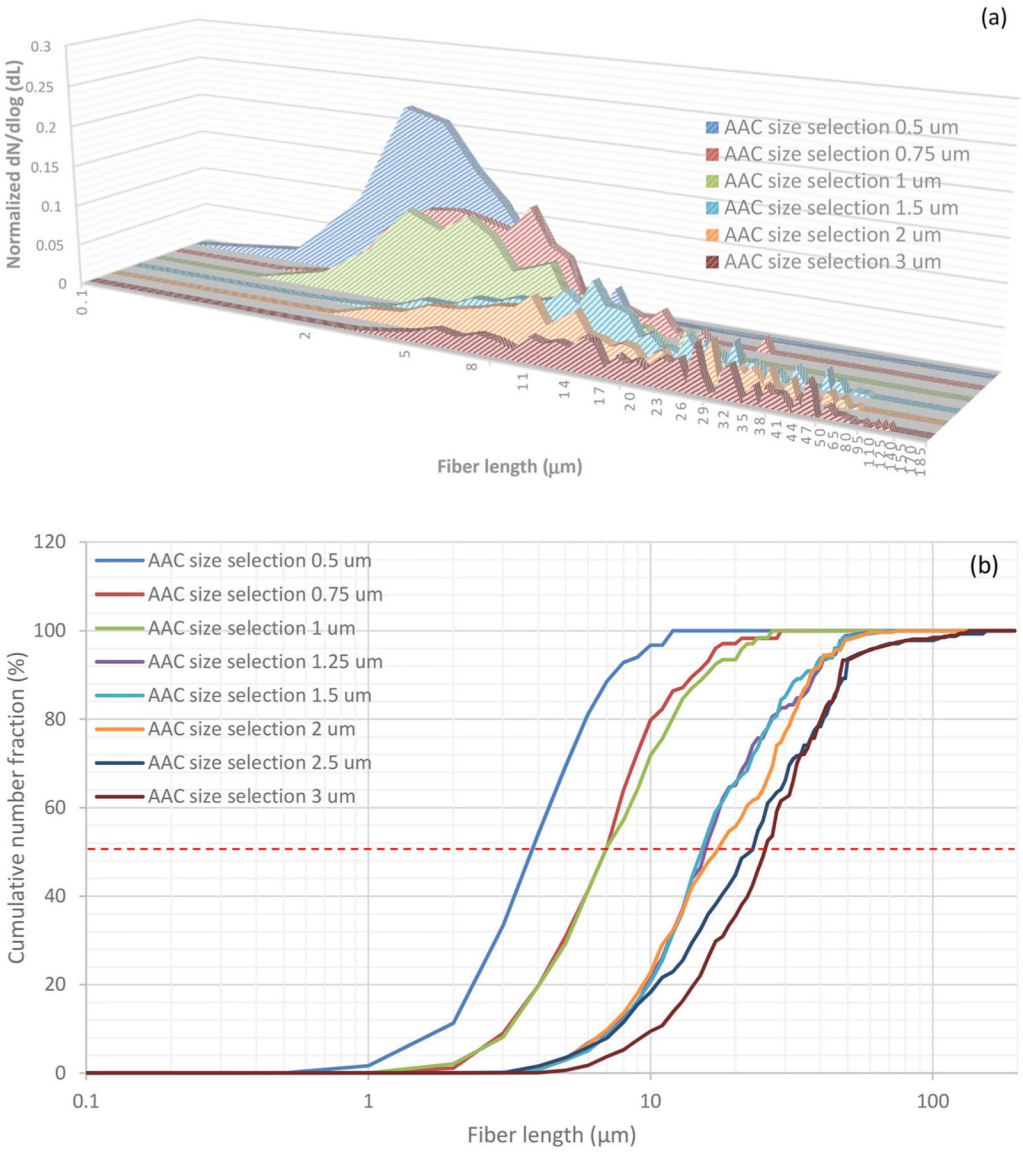

Figure 5.

Normalized particle number-weighted distribution as a function of glass fiber length (a) and cumulative number distribution as a function of glass fiber length (b).

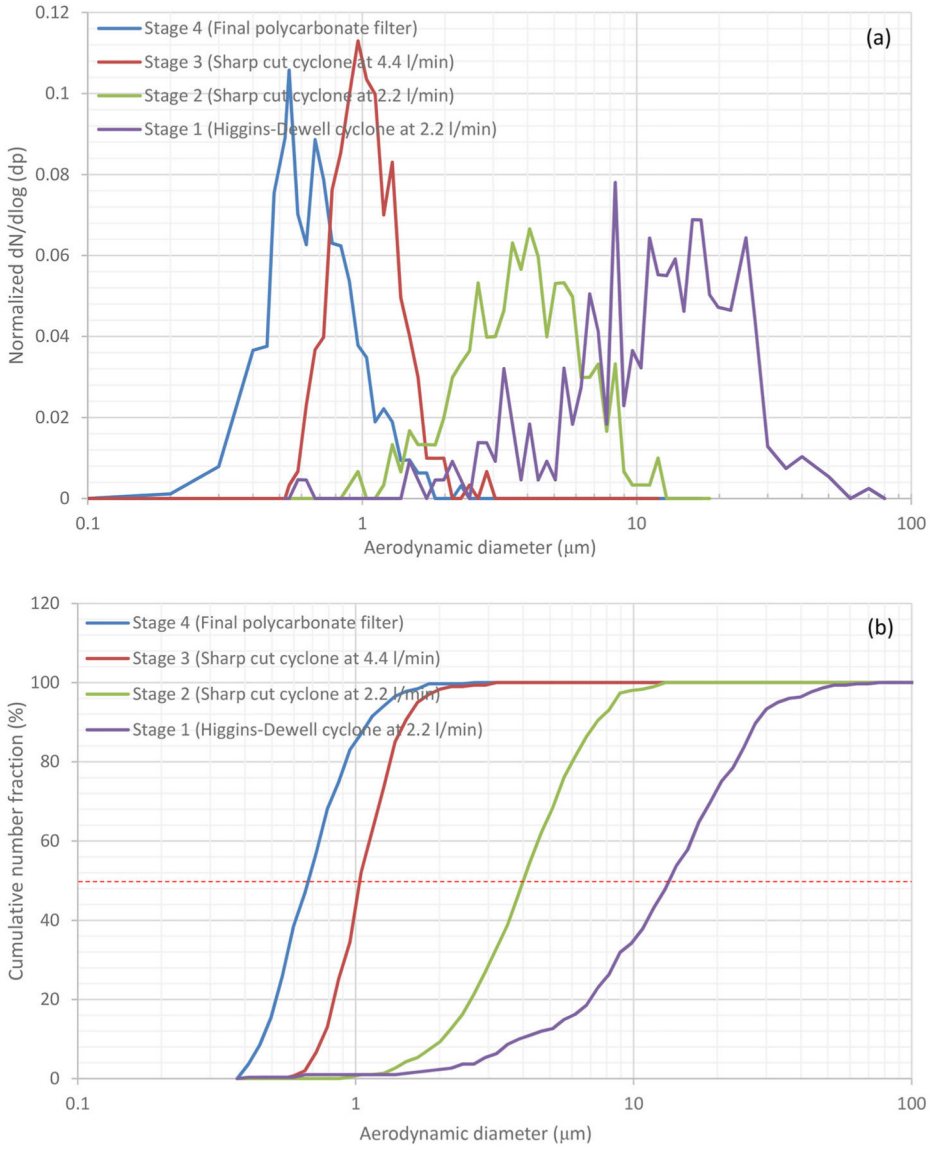

Figure 6.

Normalized particle number-weighted distribution of glass fiber aerosols collected in grit pots of the sharp cut cyclones and filter (a) and cumulative number distribution for aerodynamic diameter of glass fiber aerosols.

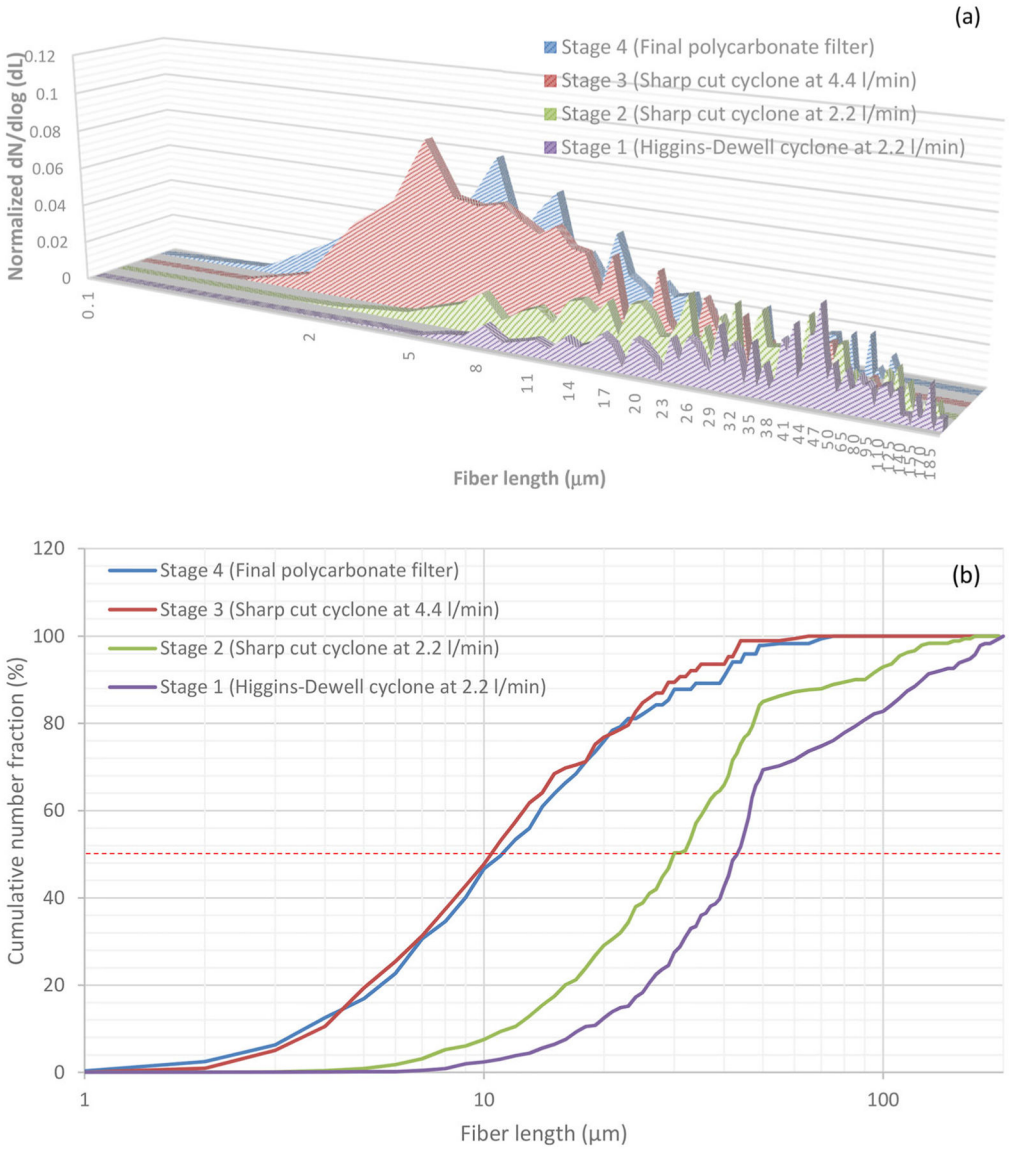

Figure 7.

Normalized particle number-weighted distribution as a function of glass fiber length collected in grit pots of the sharp cut cyclones and filter (a) and cumulative number distribution as a function of glass fiber length (b).

Table 1.

Experimental parameters of AAC for glass fiber aerosol classification.

Selected aerodynamic diameter in AAC, μm	Speed, rad/s*	Sheath flow rate, L/min	Sample flow rate, L/min
0.5	207.7		
0.75	114.6		
1.0	111.0		
1.25	90	11.36	0.3
1.5	75.7		
2.0	57.5		
2.5	46.3		
3.0	38.8		

* 1 rad/s: 9.55 revolutions per min.

Table 2.

Physical characteristics of classified glass fiber aerosols with Aerodynamic Aerosol Classifier determined by FESEM analysis.

		Fiber d_{ae}		Fiber length		Fiber width	
Selected d_{ae} [A] with AAC, μm	Sample number	GM [B], μm	GSD [C]	GM, μm	GSD	GM, μm	GSD
0.5	216	0.54	1.12	2.81	1.49	0.17	1.14
0.75	301	0.79	1.18	4.77	1.52	0.24	1.19
1	301	1.06	1.16	4.75	1.58	0.34	1.24
1.25	333	1.46	1.19	11.02	1.60	0.42	1.23
1.5	301	1.56	1.16	11.42	1.58	0.46	1.16
2	301	1.90	1.22	11.28	1.65	0.6	1.22
2.5	301	2.39	1.18	12.96	1.69	0.74	1.18
3	282	2.71	1.26	17.84	1.55	0.81	1.22

[A] Aerodynamic diameter.

[B] Geometric mean.

[C] Geometric standard deviation.

Table 3.

Average count median aerodynamic diameter, geometric standard deviation, number concentration, and mass concentration of separated glass fiber aerosols with Aerodynamic Aerosol Classifier measured with Aerodynamic Particle Sizer (APS).

Selected aerodynamic diameter with AAC, μm	Average count median aerodynamic diameter, μm	Average GSD	Average number concentration, fiber/m^3	Average mass concentration, μg/m^3
0.5	0.716	1.20	2×10^7	1.5
0.75	0.792	1.21	2.6×10^8	43
1.0	1.097	1.23	3.4×10^8	169
1.25	1.210	1.27	2.0×10^8	141
1.5	1.500	1.23	6.8×10^7	89
2.0	1.737	1.33	1.2×10^8	243
2.5	1.953	1.36	2.0×10^7	59
3.0	2.287	1.43	1.4×10^8	702

Table 4.

Physical characteristics of separated glass fiber aerosols with multi-cyclone sampling array determined by SEM analysis.

		Fiber d_{ae} [B]		Fiber length		Fiber width	
	Sample number	GM [C], μm	GSD [D]	GM, μm	GSD	GM, μm	GSD
Stage 1 (Higgins Dewell at 2.2L/min; $d_{50} \approx 4.0$ μm [A])	300	12	1.5	41.6	1.62	4.1	1.78
Stage 2 (Sharp cut cyclone at 2.2L/min; $d_{50} \approx 0.74$ μm [A])	301	3.9	1.4	21.1	1.60	1.2	1.32
Stage 3 (Sharp cut cyclone at 4.4L/min; $d_{50} \approx 0.38$ μm [A])	301	1.1	1.25	6	1.79	0.3	1.33
Stage 4 (Final polycarbonate filter)	324	0.69	1.32	5.5	1.82	0.2	1.21

[A] Cut off diameters were from Mischler et al. 2013.

[B] Aerodynamic diameter.

[C] Geometric mean.

[D] Geometric standard deviation.